

# Analytical model for optical bistability in nonlinear metal nano-antennae involving Kerr materials

Fei Zhou,<sup>1</sup> Ye Liu,<sup>1</sup> Zhi-Yuan Li,<sup>1,\*</sup> and Younan Xia<sup>2</sup>

<sup>1</sup> *Laboratory of Optical Physics, Institute of Physics, Chinese Academy of Sciences, P.O. Box 603, Beijing 100190, China*

<sup>2</sup> *Department of Biomedical Engineering, Washington University, St. Louis 63130, Missouri, USA*  
*\*lizy@aphy.iphy.ac.cn*

**Abstract:** Optical bistability at nanoscale is a promising way to realize optical switching, a key component of integrated nanophotonic devices. In this work we present an analytical model for optical bistability in a metal nano-antenna involving Kerr nonlinear medium based on detailed analysis of the correlation between the incident and extinction light intensity under surface plasmon resonance (SPR). The model allows one to construct a clear picture on how the threshold, contrast, and other characteristics of optical bistability are influenced by the nonlinear coefficient, incident light intensity, local field enhancement factor, SPR peak width, and other physical parameters of the nano-antenna. It shows that the key towards low threshold power and high contrast optical bistability in the nanosystem is to reduce the SPR peak width. This can be achieved by reducing the absorption of metal materials or introducing gain media into nanosystems.

©2010 Optical Society of America

**OCIS codes:** (240.6680) Surface plasmons; (190.1450) Bistability; (190.3270) Kerr effect.

---

## References and links

1. H. M. Gibbs, *Optical Bistability: Controlling Light with Light*, Quantum electronics—principles and applications (Academic Press, 1985)
2. H. Nihei, and A. Okamoto, "Photonic crystal systems for high-speed optical memory device on an atomic scale," *Proc. SPIE* **4416**, 470–473 (2001).
3. G. Assanto, Z. Wang, D. J. Hagan, and E. W. Vanstryland, "All-optical modulation via nonlinear cascading in type II second-harmonic generation," *Appl. Phys. Lett.* **67**(15), 2120–2122 (1995).
4. D. A. Mazurenko, R. Kerst, J. I. Dijkhuis, A. V. Akimov, V. G. Golubev, D. A. Kurdyukov, A. B. Pevtsov, and A. V. Sel'kin, "Ultrafast optical switching in three-dimensional photonic crystals," *Phys. Rev. Lett.* **91**(21), 213903 (2003).
5. G. Priem, P. Dumon, W. Bogaerts, D. Van Thourhout, G. Morthier, and R. Baets, "Optical bistability and pulsating behaviour in silicon-on-insulator ring resonator structures," *Opt. Express* **13**(23), 9623–9628 (2005).
6. F. Y. Wang, G. X. Li, H. L. Tam, K. W. Cheah, and S. N. Zhu, "Optical bistability and multistability in one-dimensional periodic metal-dielectric photonic crystal," *Appl. Phys. Lett.* **92**(21), 211109 (2008).
7. M. F. Yanik, S. H. Fan, and M. Soljagic, "High-contrast all-optical bistable switching in photonic crystal microcavities," *Appl. Phys. Lett.* **83**(14), 2739–2741 (2003).
8. M. F. Yanik, S. H. Fan, M. Soljacić, and J. D. Joannopoulos, "All-optical transistor action with bistable switching in a photonic crystal cross-waveguide geometry," *Opt. Lett.* **28**(24), 2506–2508 (2003).
9. G. A. Wurtz, R. Pollard, and A. V. Zayats, "Optical bistability in nonlinear surface-plasmon polaritonic crystals," *Phys. Rev. Lett.* **97**(5), 057402 (2006).
10. C. J. Min, P. Wang, C. C. Chen, Y. Deng, Y. H. Lu, H. Ming, T. Y. Ning, Y. L. Zhou, and G. Z. Yang, "All-optical switching in subwavelength metallic grating structure containing nonlinear optical materials," *Opt. Lett.* **33**(8), 869–871 (2008).
11. Y. Shen, and G. P. Wang, "Optical bistability in metal gap waveguide nanocavities," *Opt. Express* **16**(12), 8421–8426 (2008).
12. N. Large, M. Abb, J. Aizpurua, and O. L. Muskens, "Photoconductively loaded plasmonic nanoantenna as building block for ultracompact optical switches," *Nano Lett.* **10**(5), 1741–1746 (2010).
13. P. Mühlischlegel, H. J. Eisler, O. J. F. Martin, B. Hecht, and D. W. Pohl, "Resonant optical antennas," *Science* **308**(5728), 1607–1609 (2005).
14. O. L. Muskens, V. Giannini, J. A. Sánchez-Gil, and J. Gómez Rivas, "Strong enhancement of the radiative decay rate of emitters by single plasmonic nanoantennas," *Nano Lett.* **7**(9), 2871–2875 (2007).

15. J. W. Liaw, "Analysis of a bowtie nanoantenna for the enhancement of spontaneous emission," *IEEE J. Sel. Top. Quantum Electron.* **14**(6), 1441–1447 (2008).
  16. Y. Liu, F. Qin, F. Zhou, and Z. Y. Li, "Ultrafast and low-power photonic crystal all-optical switching with resonant cavities," *J. Appl. Phys.* **106**(8), 083102 (2009).
  17. B. T. Draine, and P. J. Flatau, "Discrete-dipole approximation for scattering calculations," *J. Opt. Soc. Am. A* **11**(4), 1491–1499 (1994).
  18. F. Zhou, Z. Y. Li, Y. Liu, and Y. N. Xia, "Quantitative analysis of dipole and quadrupole excitation in the surface plasmon resonance of metal nanoparticles," *J. Phys. Chem. C* **112**(51), 20233–20240 (2008).
  19. A. Alù, and N. Engheta, "Tuning the scattering response of optical nanoantennas with nanocircuit loads," *Nat. Photonics* **2**(5), 307–310 (2008).
  20. J. Berthelot, A. Bouhelier, C. Huang, J. Margueritat, G. Colas-des-Francis, E. Finot, J.-C. Weeber, A. Dereux, S. Kostcheev, H. I. E. Ahrach, A.-L. Baudrion, J. Plain, R. Bachelot, P. Royer, and G. P. Wiederrecht, "Tuning of an optical dimer nanoantenna by electrically controlling its load impedance," *Nano Lett.* **9**(11), 3914–3921 (2009).
  21. Z. Y. Li, and Y. N. Xia, "Metal nanoparticles with gain toward single-molecule detection by surface-enhanced Raman scattering," *Nano Lett.* **10**(1), 243–249 (2010).
- 

## 1. Introduction

It has been commonly acknowledged that all-optical devices at the micrometer and nanometer scales is a promising way towards realization of next-generation ultrafast communication and signal processing systems beyond today's microelectronics devices, which have gradually encountered limitation in bandwidth and speed. Optical switching is an essential component in the all-optical network. A feasible approach to all-optical switching is based on optical bistability, an important subject in nonlinear optics [1]. Optical bistability offers many intriguing applications, such as optical memory [2], optical transistor [3], all-optical switching [4], and among others. In recent years there has been a great interest in exploring and realizing optical bistability in nonlinear nanophotonic systems. Optical bistability has been predicted by theory or demonstrated by experimental studies to exist in waveguide-ring resonators [5], photonic crystal cavities [6–8], plasmonic crystals [9], subwavelength metallic gratings [10], metal gap waveguide nanocavities [11], and nanoantenna with amorphous silicon filled in the gap [12]. It is important to achieve a deeper understanding of the basic physics of optical bistability at the nanoscale in order to design and realize high-performance nanophotonic switching devices.

The physics of optical bistability in a classical optical resonant system such as Fabry-Perot etalon has been well established and can be described by simple analytical models [1]. However, so far a similar analytical model has not yet been available for nonlinear nanophotonic systems. Recently we successfully worked out an analytical model for describing the optical bistability of a metal nano-antenna involving a Kerr nonlinear material, which will be addressed in this letter. We propose to investigate the optical bistability of an optical nano-antenna [13–15] because this structure can provide very strong field enhancement in the center gap due to surface plasmon resonance (SPR) and the SPR peak is very sensitive to the refractive index change of the Kerr material used to fill the gap. The analytical model can help us obtain deep insight into the fundamental physics of optical bistability at nanoscale.

This paper is arranged as follows. In Sec. 2 we present a detailed process of how we reach such an analytical solution of optical bistability in the nonlinear nano-antenna structure. In Sec. 3 we briefly discuss what the analytical model can do to reveal the key factors for a deep insight of the underlying physics of optical bistability in nonlinear nanosystems. In Sec. 4 we make a brief summary of this paper.

## 2. Derivation of the analytical model

The nano-antenna structure we studied is depicted in Fig. 1. Silver is chosen as the material for the arms because of its low absorption. In the gap between the two arms, a Kerr nonlinear material is introduced. We use polystyrene with the following optical parameters: a linear refractive index  $n_0 = 1.59$ , and a Kerr nonlinear coefficient  $n_2 = 1.14 \times 10^{-12} \text{ cm}^2/\text{W}$  [16]. In our study, we are interested in the bistability between the incident optical intensity  $I_0$  and the

extinction power  $W_{ext}$ . In our simulation, the coordinates are established as shown in Fig. 1. The incident light propagates along the  $-z$ -axis, and its electric field  $\mathbf{E}$  is along the  $x$ -axis, which is a longitudinal polarization. The total length of the nano-antenna is 130 nm, and the width is 20 nm. The thickness of polystyrene embedded in the center gap is 10 nm. In the following, we will derive the analytical expressions to reveal the physical process of optical bistability.

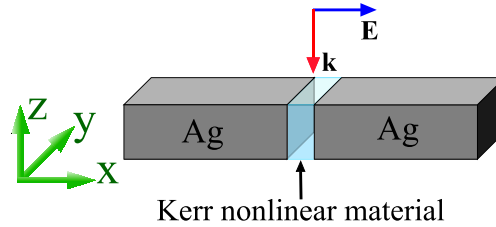


Fig. 1. Schematic structure of the nonlinear nano-antenna system.

As the first step, we temporarily disregard the nonlinear property of polystyrene. The calculated extinction spectrum is displayed in Fig. 2. The discrete dipole approximation (DDA) method [17,18] is adopted in our simulations. In Fig. 2, the black circles are the calculated extinction cross section values, showing strong SPR. The red line is the curve fitted with a Lorentz model, which can perfectly describe the extinction spectrum. The Lorentz function is

$$C_{ext} = \frac{2A}{\pi} \frac{w}{4(\lambda - \lambda_c)^2 + w^2}, \quad (1)$$

where  $C_{ext}$  is the extinction cross section,  $w$  is the full width at half maximum (FWHM) of the SPR peak,  $\lambda$  is the incident light wavelength,  $\lambda_c$  is the SPR peak wavelength, and  $A$  is a fitting parameter related to the magnitude of the peak. In our case, the fit results are  $A = 0.00625 \mu\text{m}^3$ ,  $w = 0.04903 \mu\text{m}$ , and  $\lambda_c = 0.6638 \mu\text{m}$ .

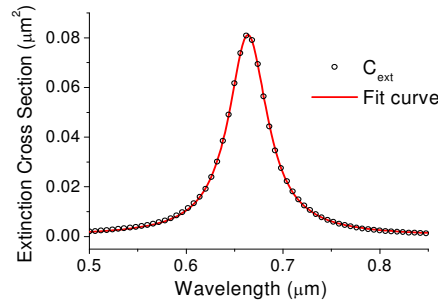


Fig. 2. Extinction spectrum of nano-antenna. Black circles are the results simulated with DDA method, and the red line is the fit curve with Lorentz function. Excellent agreement is obtained.

In order to deal with the nonlinear process, we need to study the electric field distribution in the gap. We simulate the electric field distribution at the wavelength of resonance (663.8 nm). The results are depicted in Fig. 3. The field distributions in  $yz$ -planes (Fig. 3a) and  $xy$ -planes (Fig. 3b) are both shown. Meanwhile, we give the field enhancement factor along the  $x$ -axis and  $y$ -axis as depicted in Fig. 3(c) and (d). The field enhancement factors along  $x$ -axis and  $y$ -axis with an arbitrarily selected wavelength (700 nm) are also plotted in Fig. 3(c) and (d). At both wavelengths, the electric field is quite uniform for most part in the gap except for the position very close to the edge of the silver bars. Here, we only select two wavelengths to show the property of uniform electric field in the gap, but the same results are found at other

wavelengths. So, without losing generality, the field in the gap can be considered as a uniform electric field. Consequently the refractive index change in the gap region is also considered to be uniform.

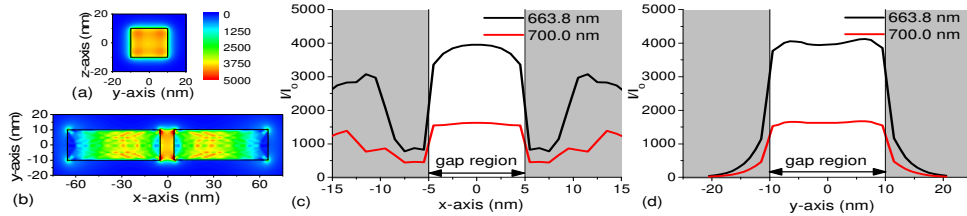


Fig. 3. Electric field distributions (in unit of  $I_0$ ) with different wavelengths of  $\lambda = 663.8$  nm:

(a)  $yz$ -plane and (b)  $xy$ -plane. (c) and (d) are the field enhancement factor  $I/I_0$  along  $x$  and  $y$  axes (the black lines). The fields for the wavelength of  $\lambda = 700$  nm are also plotted (the red lines). The electric field distribution in the gap region shows high uniformity.

As is well known, the local field enhancement in the nano-antenna is caused by SPR. The extent of SPR can be characterized by the extinction efficiency of the nanoparticle, which is proportional to  $C_{ext}$ . So the field enhancement factor  $I/I_0$  (with  $I$  being the local field intensity) is a function of  $C_{ext}$ . To get the analytical expression between  $I/I_0$  and  $C_{ext}$ , we calculate the local field enhancement factor in the gap and the extinction cross section for wavelength from 500 to 900 nm. The relationship between  $I/I_0$  and  $C_{ext}$  is shown in Fig. 4, where the black dots are for the wavelength at the left side of the resonant peak, while the red dots for the right side. At a resonant wavelength of around 664 nm, the extinction cross section is maximal, and the field enhancement factor reaches its maximum of around 4000. With the deviation away from this resonant wavelength, the electric field enhancement factor becomes lower. The overall curve in Fig. 4 can be approximately described by a linear expression:

$$I/I_0 = \beta C_{ext} \quad (2)$$

where  $\beta$  is a linear fitting parameter about  $4.906 \times 10^4 \mu\text{m}^{-2}$  for this case. The linear approximation does not influence the physical essence of the nano-antenna system and it makes possible simple analytical solution of the nonlinear bistability problem.

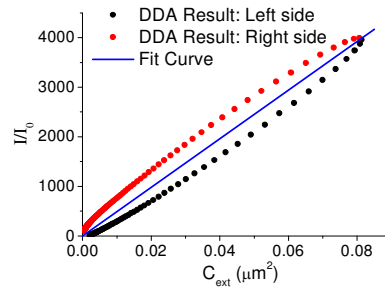


Fig. 4. Relationship between the field enhancement factor  $I/I_0$  and the extinction cross section  $C_{ext}$ . The black dots are for the wavelength at the left side of the resonant peak, while the red dots for the right side. The fit curve by a linear function is denoted as blue line.

Previous studies showed that the resonant wavelength of nano-antennae can be tuned by changing the load [19,20]. In our case, the resonant wavelength is simply tuned by the refractive index change of the Kerr material in the gap. Now we turn to study the shift of

resonant peak with different refractive indices for the central nonlinear material in details. As is shown before, the refractive index distribution in the gap can be considered uniform. So we change the refractive index in the gap region uniformly, and calculate their extinction spectra, which are shown in Fig. 5(a). As the refractive index in the gap increases, the resonant peak shifts to longer wavelengths while the shape of the extinction spectrum changes little. We extract the wavelength of resonant peak versus the refractive index in the gap region, and the result is shown in the Fig. 5(b). Very good linear relationship is found. So the peak wavelength can be expressed as  $\lambda_l = \lambda_c' + \alpha n_l$ , where  $\lambda_l$  is the resonant peak wavelength with  $n_l$ , which is the nonlinear refractive index in the gap.  $\lambda_c'$  and  $\alpha$  are the linear fit parameters. On the other hand, the nonlinear refractive index is directly proportional to the local field intensity, which is  $n_l = n_0 + n_2 I$ . So the final equation is:

$$\lambda_l = \lambda_c' + \alpha(n_0 + n_2 I) = \lambda_c + \alpha n_2 I, \quad (3)$$

In our case shown in Fig. 5,  $\alpha = 0.06379 \mu\text{m}$ .

Up to this point, we have analytical expressions for the extinction spectrum [Eq. (1)], the field enhancement factor versus the extinction cross section [Eq. (2)], and the shift of resonant wavelength under different incident intensities [Eq. (3)]. Considering that the optical bistability we study here is the relationship between the input intensity and extinction power, we transform the extinction cross section  $C_{ext}$  into the extinction power  $W_{ext}$ :

$$W_{ext} = C_{ext} I_0. \quad (4)$$

By replacing  $\lambda_c$  in Eq. (1) with  $\lambda_l$  and substituting Eqs. (2), (3) and (4) into Eq. (1), we can finally obtain the relation between  $W_{ext}$  and  $I_0$ :

$$I_0 = W_{ext} \frac{\pi}{2A} \frac{4(\lambda - \lambda_c - \alpha n_2 \beta W_{ext})^2 + w^2}{w}. \quad (5)$$

Equation (5) is the analytical expression of optical bistability between the incident intensity  $I_0$  and the extinction power  $W_{ext}$ .

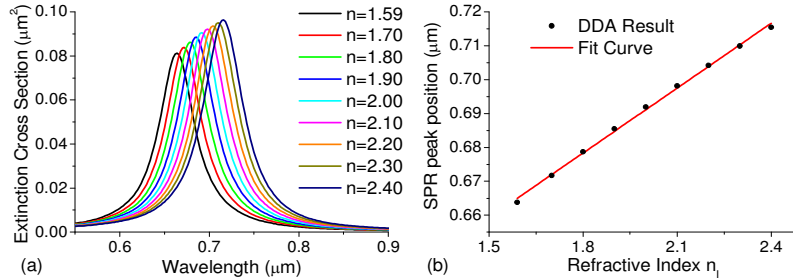


Fig. 5. (a) Shift of extinction spectra with the change of refractive index in the gap region. (b) The relationship between the SPR peak wavelength and the corresponding refractive index in the gap region. The black dots are the simulated results with DDA method, and the red line is the fitted curve. Very good linear relationship is found.

### 3. Key factors of optical bistability

Now that we have derived the analytical formalism of optical bistability in the nonlinear nano-antenna, we proceed to discuss several key factors from the analytical model. The first thing that we concern is the criterion for optical bistability. When optical bistability exists, there must be three values of  $W_{ext}$  corresponding to an incident intensity  $I_0$ . Two of them correspond to the real and stable physical states, while the other one with value in the middle

corresponds to a virtual and unstable physical state. Taking the derivative of  $I_0$  with respect to  $W_{ext}$  in Eq. (5), we can get the following expression:

$$\frac{dI_0}{dW_{ext}} = \frac{\pi}{2Aw} \left[ 4(\lambda - \lambda_c)^2 + w^2 - 16\alpha\beta n_2 (\lambda - \lambda_c) W_{ext} + 12\alpha^2 \beta^2 n_2^2 W_{ext}^2 \right]. \quad (6)$$

The condition for the existence of optical bistability is that

$$\frac{dI_0}{dW_{ext}} = 0 \quad (7)$$

has two distinct roots, which can be satisfied when

$$\Delta = 16\alpha^2 \beta^2 n_2^2 \left[ 4(\lambda - \lambda_c)^2 - 3w^2 \right] > 0. \quad (8)$$

From this equation we find that  $|\lambda - \lambda_c| > \sqrt{3}w/2$  must be satisfied to assure the existence of optical bistability in the nano-antenna system. For positive nonlinearity with  $n_2 > 0$  it means that  $\lambda > \lambda_c + \sqrt{3}w/2$ , while for negative nonlinearity with  $n_2 < 0$  we must have  $\lambda < \lambda_c - \sqrt{3}w/2$ . In our nano-antenna structure, the resonant peak is located at around 664 nm with FWHM of about 49 nm. So the critical condition for optical bistability becomes  $\lambda_l > 705$  nm.

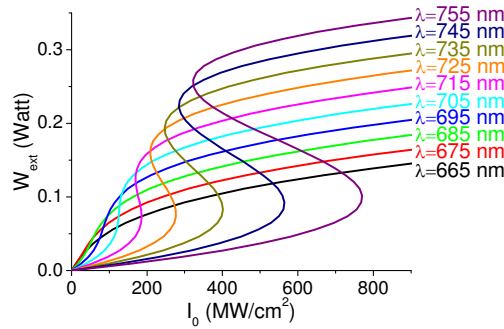


Fig. 6. Relationship between the extinction power and the incident intensity at different wavelengths. The  $W_{ext}$  is peak extinction power.

We plot the extinction powers versus the incident intensities at different wavelengths in Fig. 6. Each color represents an individual incident wavelength. From the figure, we can find that the critical wavelength for bistability is somewhere between 705 nm (the cyan line) and 715 nm (the magenta line). For shorter incident wavelengths than the critical wavelength, there are no bistable states; while for longer ones, the bistable states can be observed. The total refractive index change of the Kerr material required to maintain optical bistability is on the order of 0.1.

The above analytical model can provide much more information than the criterion of optical bistability. We can get the two roots of Eq. (7) directly as:

$$\begin{aligned} W_{ext,1} &= \frac{2(\lambda - \lambda_0)}{3\alpha\beta n_2} (1 - \sqrt{1-p}), \\ W_{ext,2} &= \frac{2(\lambda - \lambda_0)}{3\alpha\beta n_2} (1 + \sqrt{1-p}), \end{aligned} \quad (9)$$

where  $p = \frac{3w^2}{4(\lambda - \lambda_0)^2}$ . The corresponding incident intensity can be obtained by substituting Eq. (9) into Eq. (5):

$$\begin{aligned} I_1 &= \frac{8\pi(\lambda - \lambda_0)^3}{27A\alpha\beta n_2 w} \left[1 - \sqrt{1-p}\right] \cdot \left[1 + p + \frac{1}{2}\sqrt{1-p}\right], \\ I_2 &= \frac{8\pi(\lambda - \lambda_0)^3}{27A\alpha\beta n_2 w} \left[1 + \sqrt{1-p}\right] \cdot \left[1 + p - \frac{1}{2}\sqrt{1-p}\right]. \end{aligned} \quad (10)$$

$(I_1, W_{ext,1})$  and  $(I_2, W_{ext,2})$  are the two critical points of the bistability curves, and  $I_1$  represents the threshold power of optical bistability at a given incident wavelength. The contrast of bistability signal is characterized by

$$\frac{W_{ext,2} - W_{ext,1}}{(W_{ext,2} + W_{ext,1})/2} = \sqrt{1-p}, \quad (11)$$

and

$$\frac{I_2 - I_1}{(I_2 + I_1)/2} = \frac{2(1-p)^{3/2}}{1+p}. \quad (12)$$

It is seen that the contrasts of both  $I$  and  $W_{ext}$  are only dependent on the parameter  $p$ . To increase the contrast of the two states, the only choice is either to make the resonant peak narrower or to select an incident wavelength farther away from the resonant wavelength. On the other hand, as shown in Eq. (10), the threshold intensity is inversely proportional to  $A$ ,  $\alpha$ ,  $\beta$ , and  $n_2$ , which means that the pump intensity can be decreased with larger  $A$ ,  $\alpha$ ,  $\beta$ , and  $n_2$ . In other words, the threshold pump power can be reduced by increasing the magnitude and sensitivity of the SPR peak, the local field enhancement factor, and the Kerr nonlinear coefficient.

The maximum enhancement factor at the resonant wavelength is nearly 4000 for the nano-antenna, which can reduce the threshold power efficiently. However, the FWHM of extinction spectrum is relatively large as nearly 50 nm. This is the main problem for low-power and high-contrast optical bistability with nano-antenna according to the above analytical model. The threshold power is around 800 MW/cm<sup>2</sup> at wavelength 755 nm. If a lower threshold power needs to be implemented, the extinction spectrum with SPR should be narrower.

Our previous study shows that the line width of extinction spectrum is closely related the absorption of metal nanoparticles [21]. If the absorption of a metal material is reduced, the line width of the SPR peak can be compressed. One way to achieve this is to shift the operation wavelength of optical functionality to longer wavelengths. Another way is to take a metal material with smaller intrinsic absorption. Here we propose an alternative way. Moreover, it has been shown that a proper gain, which can be supplied by fluorescence molecules or quantum dots, can effectively compensate for the absorption of metal, and lead to a very narrow spectrum width [21]. We calculate the extinction spectra of the nano-antenna with different gain coefficient  $k$  in the gap region, where the medium has a complex refractive index of  $n_l - ik$ . The results are shown in Fig. 7(a). With the gain medium, the line width of extinction spectra reduces significantly. At  $k = 0.25$ , the line width decreases to about 12.5 nm, a quarter of the value without gain. In addition, the introduction of a gain medium does not influence the position of extinction peak and the speed at which the peak shifts when the refractive index is changed. It just compresses the line width of extinction spectrum. In Fig. 7(b), we show the relationship between the line width and the gain

coefficient. When  $k$  grows from zero to 0.25, the line width narrows nearly linearly. The calculation results of the optical bistability curve with  $k = 0.25$  are displayed in Fig. 7. We find that the threshold power is reduced to only  $7 \text{ MW/cm}^2$  at a wavelength of 683 nm, and the necessary total refractive index change of the Kerr material requested to maintain optical bistability is reduced to a level on the order of 0.01.

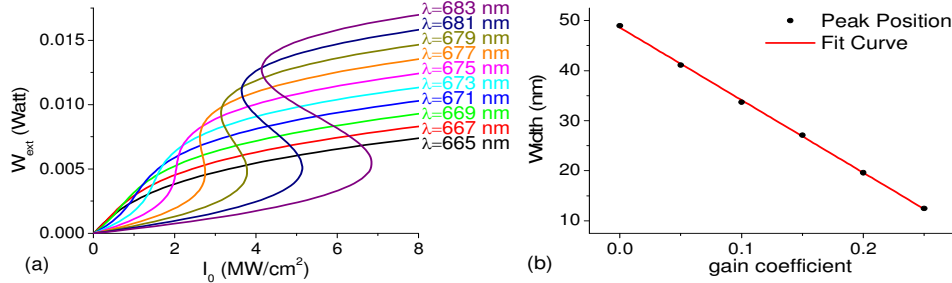


Fig. 7. (a) Optical bistability curves at different wavelengths with a gain coefficient of  $k = 0.25$  for the material in the gap. (b) The dependence of SPR peak width on the gain coefficient.

#### 4. Conclusions

In summary, we have presented an analytical model for the optical bistability in a nonlinear metal nano-antenna structure. The model clearly reveals how the performance of bistability is correlated with the physical properties of the nanosystem. According to the model, the key towards optical bistability of low pump power and high contrast is to reduce the SPR peak width of the nanosystems by designing appropriate nanosystems with low absorption or with gain. Our study can help to explore nonlinear nanophotonic systems for applications in compact low-power bistable all-optical devices and storage.

#### Acknowledgment

This work was supported by the National Natural Science Foundation of China (NNSFC) under grants 60736041 and 10874238, and the National Key Basic Research Special Foundation of China under grant 2006CB302901.